SUPPORTING INFORMATION

^{19}F Dark-State Exchange Saturation Transfer NMR Reveals Reversible Formation of Protein-Specific Large Clusters in High Concentration Protein Mixtures

John M. Edwards [1], Jack E. Bramham [1], Adrian Podmore [2], Steven M. Bishop [3], Christopher F. van der Walle [2], Alexander P. Golovanov [1*]

[1)] Manchester Institute of Biotechnology and School of Chemistry, Faculty of Science and Engineering, The University of Manchester, Manchester M1 7DN, United Kingdom.

[2)] Dosage Form Design & Development, AstraZeneca plc, Granta Park, Cambridge CB21 6GH, United Kingdom.

[3)] Biopharmaceutical Development, AstraZeneca plc, Gaithersburg, Maryland 20878, United States.

* Correspondence to: a.golovanov@manchester.ac.uk

TABLE OF CONTENTS

The pulse sequence for ^{19}F DEST experiment (for Bruker) and the MATLAB DEST fitting script with example data are provided separately as zipped folders.

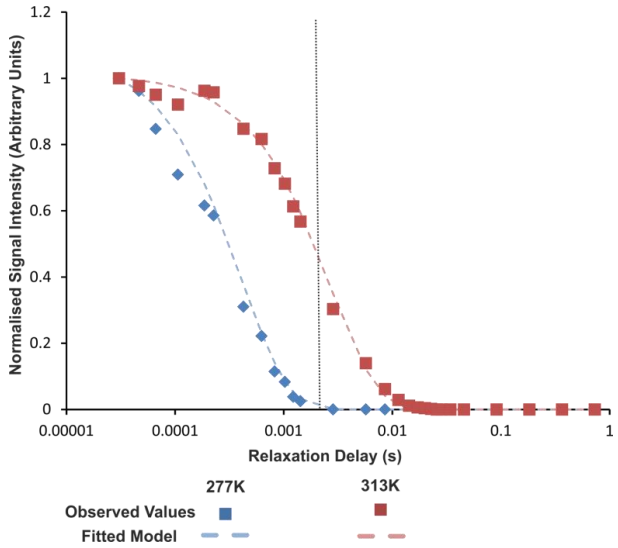

FIGURE S1: Examples of intensity decay curves from a combined pair of R_2 relaxation experiments. These consist of one experiment covering T_2 relaxation delays of 2.8 ms to 730 ms while varying the number of echo pulses separated by fixed echo delays, and an additional identical experiment in which the number of echo pulses was fixed at the minimum and the echo delay was decreased incrementally to produce effective delay times of between 1.5 and 0.03 ms. Data points from both experiments were combined and fitted simultaneously using Dynamics Center 2.4.8 to extract the single 'observed' R_2^{obs} value. X-axis is logarithmic. Data is for mAb2-TFBPD at 400 mg/mL total mAb concentration, shown for temperatures of 277K and 313K. This sample at 277K had the most rapid relaxation measured in this study. The black dotted line indicates the join between the data from the modified NMR experiment for ultra-fast relaxation (left) and the conventional CPMG experiment (right).

$$\frac{d}{dt}\begin{bmatrix} E/2 \\ I_x^A \\ I_y^A \\ I_z^A \\ I_x^B \\ I_y^B \\ I_z^B \end{bmatrix} = -\begin{bmatrix} 0 & 0 & 0 & 0 & 0 & 0 & 0 \\ 0 & R_2^A + k_{AB}^{app} & \Omega^A & -\omega_y & -k_{BA} & 0 & 0 \\ 0 & -\Omega^A & R_2^A + k_{AB}^{app} & \omega_x & 0 & -k_{BA} & 0 \\ -2\theta^A & \omega_y & -\omega_x & R_1^A + k_{AB}^{app} & 0 & 0 & -k_{BA} \\ 0 & -k_{AB}^{app} & 0 & 0 & R_2^B + k_{BA} & \Omega^B & -\omega_y \\ 0 & 0 & -k_{AB}^{app} & 0 & -\Omega^B & R_2^B + k_{BA} & \omega_x \\ -2\theta^B & 0 & 0 & -k_{AB}^{app} & \omega_y & -\omega_x & R_1^B + k_{BA} \end{bmatrix} \times \begin{bmatrix} E/2 \\ I_x^A \\ I_y^A \\ I_z^A \\ I_x^B \\ I_y^B \\ I_z^B \end{bmatrix}$$

FIGURE S2: Bloch-McConnell matrix used for modelling the DEST effect for exchange between NMR-visible species *A* and the dark state *B*; where E is unity; k_{AB}^{app} and k_{BA} are the apparent forward association and reverse dissociation rate constants, respectively; I_x^n, I_y^n, I_z^n are the equilibrium magnetisation in the x, y, and z axis, respectively, with I_z^n dependent upon equilibrium state populations ($P^A = P^{vis}$ and $P^B = P^{dark}$); R_1^n and R_2^n are the longitudinal and transverse relaxation rates, respectively; $\theta^n = R_1^n \times I_z^n$, Ω^n is the saturation frequency offset in rad·s^{-1}; and ω_x and ω_y are the CW saturation field strength (γB1) (rad·s^{-1}) about the x and y axis, respectively. Lifetime line broadening was calculated as R_2^{obs} - R_2^{mon}, providing an estimate of k_{AB}^{app} at each condition, with $k_{BA} = k_{AB}^{app} \times \frac{P^A}{P^B}$. Model parameters P^A (= P^{vis}), P^B (= P^{dark}) = 1 − P^A, and R_2^B (=R_2^{dark}) were fitted to experimental profiles using an in-house Matlab script, which minimises the difference between experimental and simulated DEST profiles for the two or three saturation field strengths simultaneously. Fitting uncertainties for the model parameters were computed using Monte-Carlo simulations, with uncertainties of derived parameters calculated by error propagation.

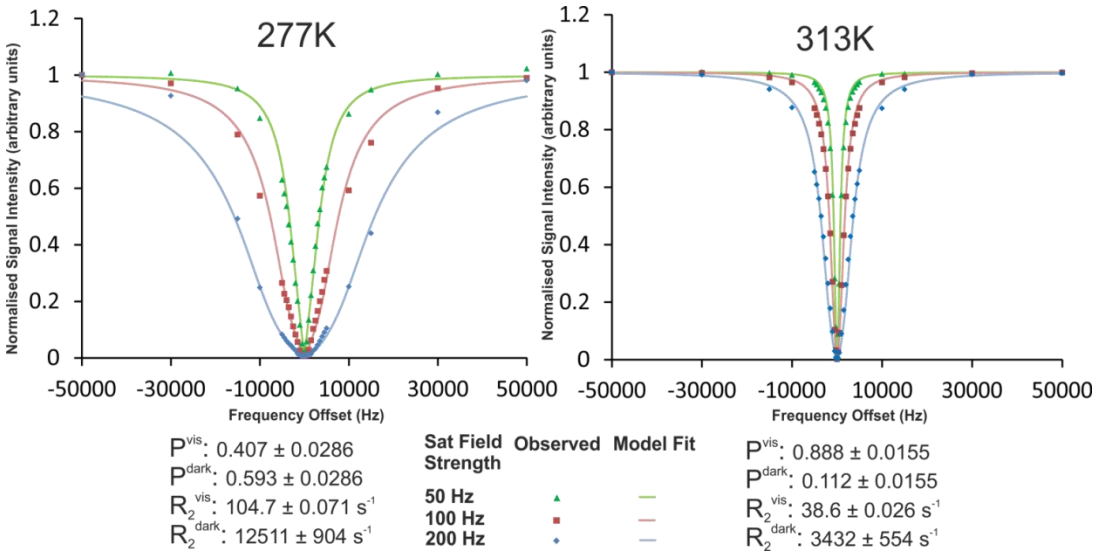

FIGURE S3: Further examples of DEST models fitted to observed data. Examples shown are for mAb2-TFBPD in a 400 mg/mL equimolar sample (200 mg/mL mAb2-TFBPD, 200 mg/mL COE19-TFCS). Data collected at 277K and 313K, at three saturation fields: 50 Hz, 100 Hz, 200 Hz. R_2^{mon} value of 38.6 ± 0.03.

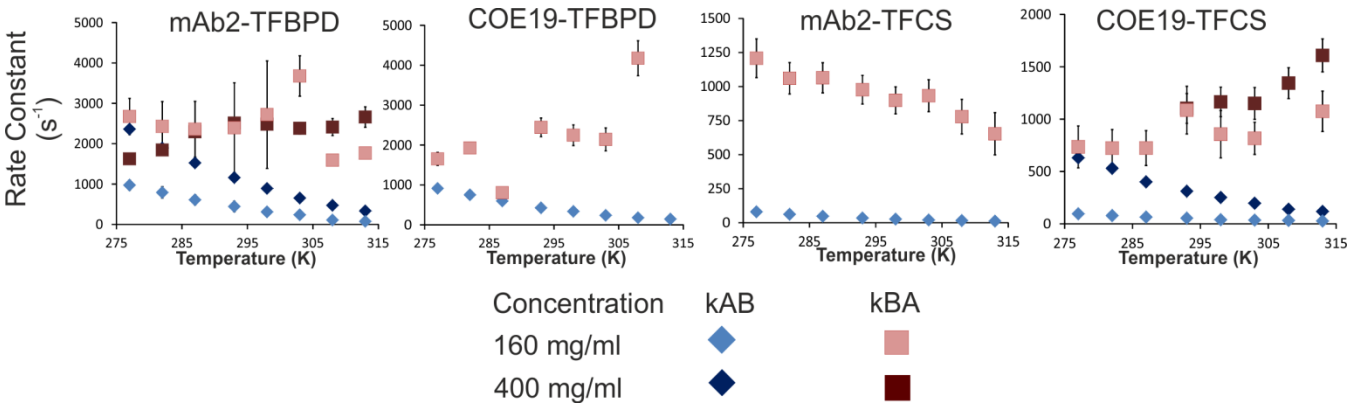

FIGURE S4: Rate constant data for two mAbs at different temperatures. The value of k_{AB}^{app} at each condition was derived from lifetime line broadening calculated as R_2^{obs} - R_2^{mon}, with $k_{BA} = k_{AB}^{app} \times \frac{P^A}{P^B}$.

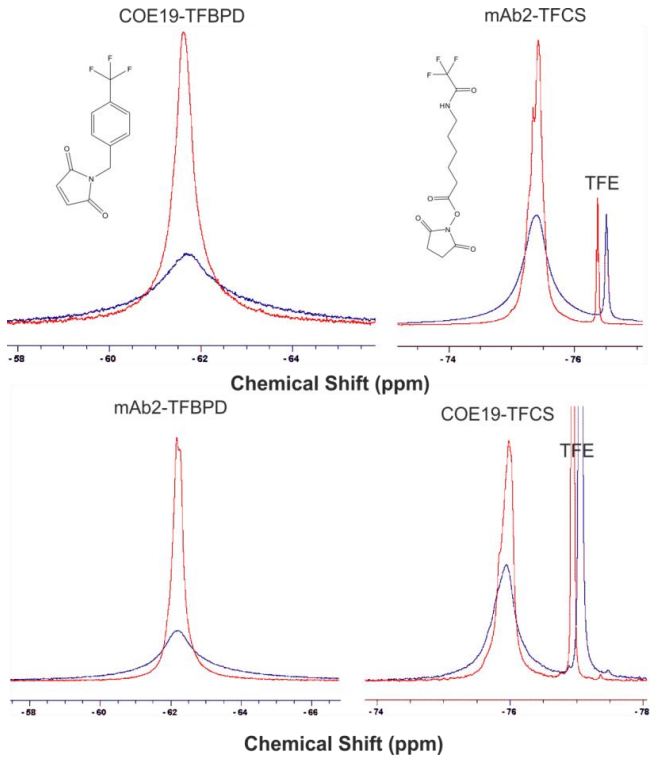

FIGURE S5: Overlays of the 1D ^{19}F NMR spectra for the four mAb-Tag combinations at 277K (in blue) and 313K (in red). Each peak is shown on the same scale at the two temperatures, but different mAb-Tag combinations are not to scale due to differences in labelling efficiency and hence absolute signal intensity. Spectra chemical shifts have been aligned so mAb peaks are directly overlaid. The additional signal visible at around 76.5ppm is from the small molecule trifluoroethanol (TFE) added as an internal reference to check dilution accuracy.

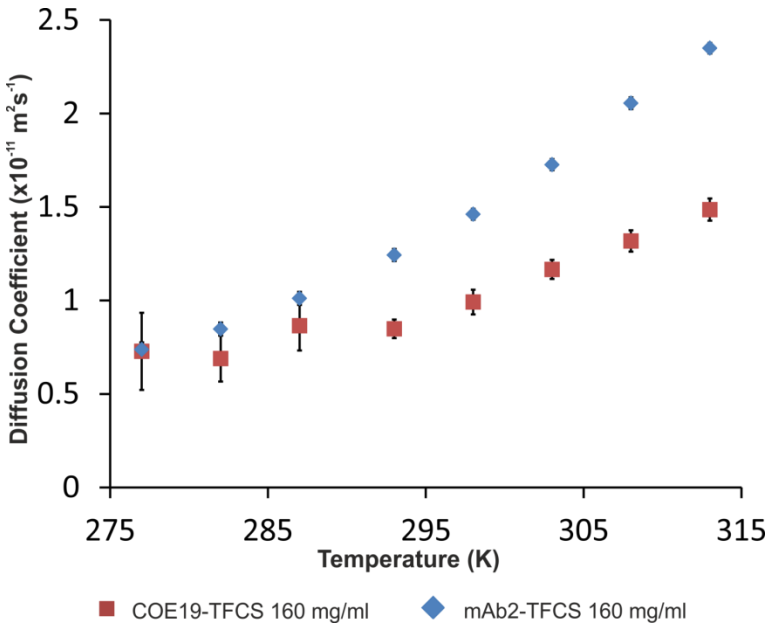

FIGURE S6: Raw diffusion coefficients D_L for both mAbs tagged with TFCS. Data is for 160 mg/mL total mAb concentration samples. Data could not be collected for TFBPD tagged mAbs, or at higher concentration, as rapid relaxation resulted in complete loss of signal before measurable diffusion could occur.

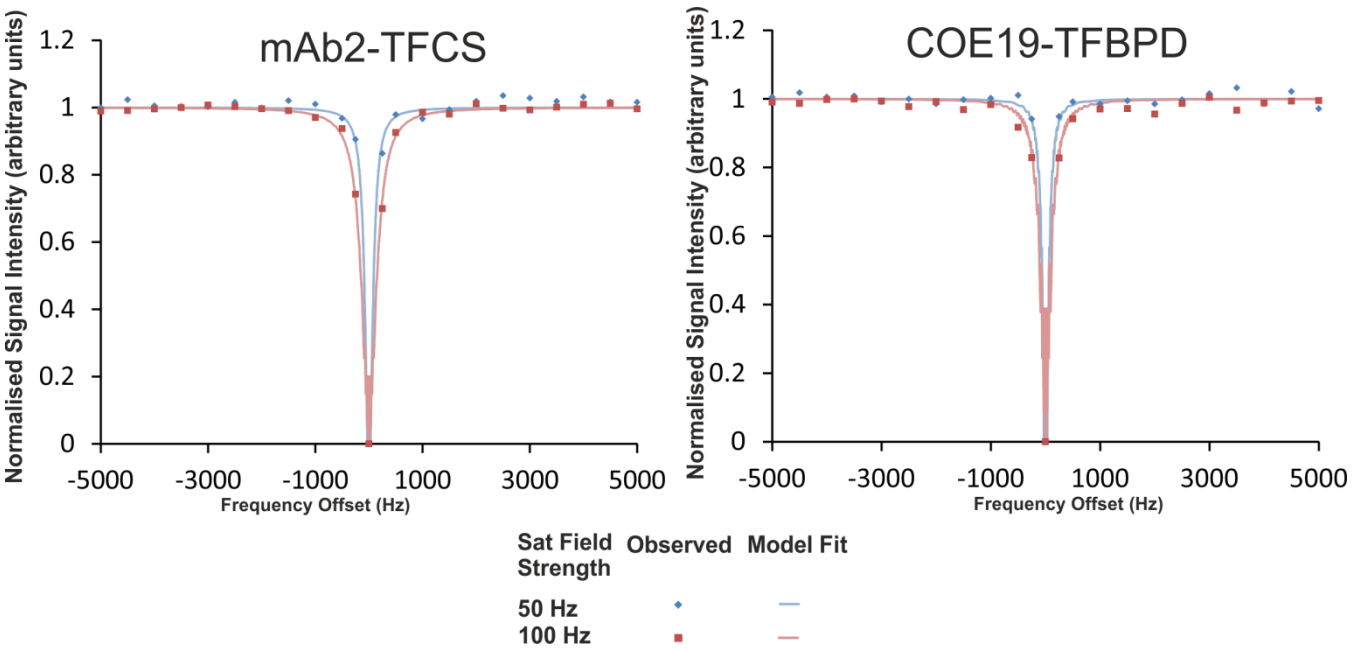

FIGURE S7: DEST model, with fixed P^{vis} = 0.99999 (i.e. no dark state population) simulated for experimental data of an equimolar sample of mAb2-TFCS and COE19-TFBPD completely denatured with 6M GdnHCl. Relaxation rates $R_2^A = R_2^{mon}$ corresponding to monomeric states of mAb2-TFCS and COE19-TFBPD in these experiments were also measured in the presence of 6M GdnHCl (1.83 and 3.41 s^{-1} for mAb2-TFCS and COE-TFBPD, respectively). Data was collected at 313K, in a 3 mm NMR tube.